PROCEEDINGS OF SCIENCE

CALET Search for electromagnetic counterparts of gravitational waves in O4

Yuta Kawakubo,[a,*] **Michael L. Cherry**[a] **and Takanori Sakamoto**[b] **for the CALET collaboration**

[a] *Department Physics & Astronomy, Louisiana State University, 202 Nicholson Hall, Baton Rouge, LA 70803, USA*

[b] *College of Science and Engineering, Department of Physics and Mathematics, Aoyama Gakuin University, 5-10-1 Fuchinobe, Chuo, Sagamihara, Kanagawa 252-5258, Japan*

E-mail: kawakubo1@lsu.edu

The latest LIGO/Virgo/KAGRA observing run (O4) started on May 24 in 2023. Many ground and space instruments have participated in follow-up observation and search for electromagnetic counterparts of gravitational waves. Calorimetric Electron Telescope (CALET) on the International Space Station has also searched for electromagnetic counterparts since the observation started in October 2015. Although CALET is a payload for direct measurement of high-energy cosmic rays, CALET has the capability to observe high-energy gamma-rays above 1 GeV with the Calorimeter (CAL) and X-rays / gamma rays in the energy range from 7 keV to 20 MeV with the CALET Gamma-ray Burst Monitor (CGBM). We searched for electromagnetic counterparts of gravitational wave events in the last LIGO/Virgo observing run (O3). Although no candidate was found in CALET data in O3, CAL and CGBM estimated upper limits of gamma-ray / X-ray flux for the gravitational waves in O3. We have been searching for electromagnetic counterparts of gravitational waves in O4 with improved and automated analysis pipelines to deal with many events with high event rates. As of the end of June 2023, the LIGO/Virgo/KAGRA collaboration reported 169 events via the GCN/LVC NOTICE, and 15 of 169 events were reported to GCN Circulars as significant events. Although CGBM and CAL searched for signals associated with the significant events, no candidates were found around the event time of the significant events. We obtained CAL upper limits for eight significant events of which localization high probability region overlapped with the CAL field of view.

38th International Cosmic Ray Conference (ICRC2023)
26 July - 3 August, 2023
Nagoya, Japan

*Speaker

1. Introduction

The latest LIGO/Virgo/KAGRA observing run (O4) started on May 24, 2023 following the engineering run (ER15) from one month before the O4 started. Much attention has been drawn to gravitational wave observation in O4, and various space and ground experiments have performed follow-up observation, and search for counterparts of gravitational waves. Although many gamma-ray burst (GRB) instruments have continued to search for short GRBs associated with binary neutron star mergers, GW 170817/GRB 170817A is still the only case of the association between a binary neutron star merger and short GRB[1–4]. As well as other GRB instruments, CALorimetric Electron Telescope (CALET) also has performed the search for electromagnetic counterparts of the gravitational waves to observe the next case of the short GRB associated with the binary neutron star merger [5–11]. CALET is a payload on the International Space Station (ISS) and has been in flight operation to observe cosmic rays and gamma rays since October 2015. CALET has the CALET Gamma-ray Burst Monitor (CGBM), which consists of two kinds of scintillation detectors, Hard X-ray Monitor (HXM) and Soft Gamma ray Monitor (SGM), to observe GRBs and other X-ray, gamma-ray transients [12]. CGBM has been monitoring the sky with X-rays and gamma rays in the energy range from 7 keV to 20 MeV. CGBM detected more than 327 GRBs, including 9 % of short GRBs, thanks to the onboard trigger system, which calculates signal-to-noise ratio every 0.25 seconds and judges the detection of transients on board [13]. Also, CALorimeter (CAL) has been collecting gamma-ray data above 1 GeV [14–16]. CALET has the possibility to detect a prompt emission and high energy gamma-ray emission of short GRBs associated with binary neutron star mergers thanks to two kinds of detectors. This paper will describe the CALET observation and analysis in O3. Also, we will present the current status of the CALET observation in O4.

2. Observation in O3

In the last observing run (O3), 56 gravitational events and one sub-threshold event were reported via GraceDB and the General Coordinates Network (GCN) [17, 18]. Since CALET was in nominal operation during the O3, we searched for electromagnetic counterparts of gravitational waves in O3. Although no candidates of electromagnetic counterparts were found in CALET data in O3, we estimated the upper limits of gamma-ray flux with CAL and CGBM data [11]. The summary of CALET observation in O3 is shown in Table 3. "Event ID," "Possible source," and Event Time were referred to GraceDB and the GCN/LVC NOTICE [17, 18]. If "Possible source" showed probabilities of multiple sources on GraceDB, the highest probability source was shown in Table 3.

CGBM collected two types of monitor data, the Pulse Height (PH) data, and the Time History (TH) data, except at the high latitude and around the South Atlantic Anomaly. Also, CGBM has an onboard trigger system to detect increased count rates by calculating the signal-to-noise ratio using Formula (1).

$$\mathrm{SNR} = \frac{N_{\mathrm{tot}} - \frac{N_{\mathrm{BG}}}{\Delta t_{\mathrm{BG}}}\Delta t}{\sqrt{\frac{N_{\mathrm{BG}}}{\Delta t_{\mathrm{BG}}}\Delta t}} \quad . \tag{1}$$

Here Δt is the foreground (signal) integration time; $N_{\rm tot}$ is the number of counts integrated over Δt in the selected energy range; and $N_{\rm BG}$ is the number of background counts in the selected energy range integrated over the background time interval $\Delta t_{\rm BG}$ preceding Δt. In the onboard trigger system, SNRs are calculated continuously every 0.25 seconds for $\Delta t_{\rm BG}$ = 16 s and four signal integration times (Δt = 0.25 s, 0.5 s, 1 s, or 4 s) over the energy ranges 25 - 100 keV for HXM and 50 - 300 keV for SGM. Onboard trigger thresholds are set at SNR = 8.5 for each HXM and 7.0 for SGM. Once any SNRs exceed the thresholds, event data are captured, and a GCN/CALET NOTICE is distributed via GCN after the automatic ground analysis. No onboard trigger occurred within $T_0\pm$ 60 seconds for each gravitational wave event, where T_0 is the event time of the gravitational wave event shown in Table 3. Since the onboard trigger system searches for signals with only limited conditions and is disabled when the event data file buffer is full, we searched for electromagnetic counterparts in the TH data for $T_0 \pm 60$ seconds in ground analysis. TH data has eight energy channels (four channels in High Gain and four channels in Low Gain) with 0.125 seconds resolution for each detector. The typical energy ranges of TH channels are shown in Table 1. We applied Formula (1) to TH data with 1440 combinations of conditions shown in Table 2. While the background time interval $\Delta t_{\rm BG}$ is taken from before Δt in the case of the onboard trigger, $\Delta t_{\rm BG}$ was taken from both sides of Δt in the case of ground analysis except near the sequence of the high voltages turning on and off. In the ground analysis, we set the threshold at SNR = 7 and require that the signal is detected by multiple detectors (HXM1, HXM2, and SGM) and in multiple energy bands. The search with TH data was performed if the CGBM high voltages were on at T_0 and the summed LIGO/Virgo localization probability $P_{\rm h}$ above the earth horizon at T_0 was greater than 1 %. The CGBM observation results were shown as "CGBM Observation." "No detection" means the search was performed; however, there were no candidates. "HV off" means the CGBM high voltages were off at T_0 and and "Outside" means $P_{\rm h}$ was less than 1%. We searched for signals associated with 34 of 57 events. Although no candidate was found in CGBM data, we estimated upper limits for the X-ray/gamma-ray flux, assuming a typical short GRB spectrum and duration. The CGBM upper limits and detail of CGBM observation and analysis in O3 is available in [11].

CAL collected data with the nominal scheduled operation during O3. For the CAL gamma-ray analysis, we use data collected in the high energy trigger (HE) mode and low energy gamma-ray (LEG) mode for analysis for above 10 GeV and 1 GeV, respectively. While the HE mode is always enabled, the LE mode is enabled only at low latitudes or during short intervals after the CGBM onboard trigger. We searched for electromagnetic counterparts in CAL data according to the method described in [9, 11]. We searched for gamma-ray events in $T_0\pm$ 60 s for each gravitational wave event if "Coverage," which is the overlapping region of the LIGO/Virgo localization map covered by the CAL field of view during the interval $T_0\pm$ 60 s, is equal or greater than 5%. "Run mode" shows the data used for the search, and we searched for gamma-ray events in 1 GeV - 10 GeV and 10 GeV - 100 GeV for LEG and HE, respectively. Although we searched for gamma-rays associated with 20 gravitational wave events of which "Coverage" equals or exceeds 5%, no candidate was found in CAL data. In the case of no candidate, gamma-ray flux upper limits were calculated for the time interval $T_0\pm$ 60 s for the energy range 10-100 GeV (HE mode) or 1-10 GeV (LEG mode). We estimated a 90 % confidence level upper limit on the gamma-ray flux based on 2.44 events above the expected negligible background, assuming a power-law spectrum with a single power-law photon index of -2 considering the CAL sensitivity. Figure 1 shows the 90 % confidence level upper limit

TH channel	HXM	SGM
High gain ch0	7 - 10 keV	40 - 100 keV
High gain ch1	10 - 25 keV	100 - 230 keV
High gain ch2	25 - 50 keV	230 - 450 keV
High gain ch3	50 - 100 keV	450 - 1000 keV
Low gain ch0	60 - 100 keV	550 - 830 keV
Low gain ch1	100 - 170 keV	830 - 1500 keV
Low gain ch2	170 - 300 keV	1.5 - 2.6 MeV
Low gain ch3	300 - 3000 keV	2.6 - 28 MeV

Table 1: Energy ranges of TH channels

Number of conditions		Conditions
detector	3	HXM1, HXM2, SGM
gain	2	High, Low
channels	10	ch0, ch1, ch2, ch3, ch0-1, ch1-2, ch2-3, ch0-2, ch1-3, ch0-3
Δt	6	1/8 s, 1/4 s, 1/2 s, 1 s, 2 s, 4 s
$\Delta t_{\rm BG}$	4	8 s, 16 s, 32 s, 64 s

Table 2: Conditions for SNR calculation

map during the interval $T_0\pm$ 60 s for S190408an. Upper limits were calculated for any directions in each pixel and shown as the color map. We obtained upper limit maps for the other 19 events, and the maximum time-averaged flux for an individual pixel in the LIGO/Virgo localization area is listed as "90% Upper limit" in Table 3.

3. Observation in O4

CALET has been searching for electromagnetic counterparts in O4 as well as O3. We have improved analysis pipelines looking toward the search for signals associated with gravitational wave events in O4. In the O3, analysis was not automated, and humans were in the process of analyzing CGBM and CAL data for every gravitational wave event. Since a higher event rate was expected than O3 and 169 gravitational events were reported by the end of June 2023, we automated CAL and CGBM analysis pipelines. Once a GCN/LVC NOTICE is distributed via GCN Kafka and the analysis server receives the notice for each event, notice information, including the event name, event time, URL to the sky map FITS data, etc., are stored as a text file in the analysis server. If any text files and high-level data are available, two pipelines for CGBM and CAL analysis process the high-level data for the quick-look analysis. Also, quick-look analyses are uploaded to the internal web server to check results easily and quickly by collaborators. Although the analysis pipeline checks the GCN/LVC NOTICE every 15 minutes, observation data are distributed hourly, and processing high-level data takes several hours. Therefore, the quick-look analysis takes at least several hours once the GCN/LVC NOTICE is distributed. Only CGBM results are publicly available on the CALET web page after a human confirms the CGBM result and uploads the source

Event ID	Possible source	Event time (T_0)	CGBM Observation	$P_{\rm h}$	$P_{\rm cal}$	Run mode	90 % Upper limit [erg s^{-1} cm^{-2}]
S190408an	BBH (>99 %)	18:18:02.288180	No detection	100%	95 %	LEG	3.0×10^{-7}
S190412m	BBH (>99 %)	05:30:44.165622	HV off	-	-	-	-
S190421ar	BBH (97 %)	21:38:56.250977	Outside	0%	0%	-	-
S190425z	BNS (>99 %)	08:18:05.017147	HV off	-	10%	HE	8.5×10^{-5}
S190426c	Terrestrial (58 %)	15:21:55.336540	HV off	-	10%	HE	9.2×10^{-6}
S190503bf	BBH (96 %)	18:54:04.294490	HV off	-	25%	HE	7.1×10^{-5}
S190510g	Terrestrial (58 %)	02:59:39.291636	No detection	16%	0%	-	-
S190512at	BBH (99 %)	18:07:14.422363	No detection	100%	0%	-	-
S190513bm	BBH (94 %)	20:54:28.747089	No detection	100%	15%	LEG	4.5×10^{-5}
S190517h	BBH (98 %)	05:51:01.830582	No detection	86%	0%	-	-
S190519bj	BBH (96 %)	15:35:44.397949	No detection	100%	0%	-	-
S190521g	BBH (97 %)	03:02:29.447266	HV off	-	30%	HE	7.4×10^{-7}
S190521r	BBH (>99 %)	07:43:59.463379	HV off	-	0%	-	-
S190602aq	BBH (>99 %)	17:59:27.089355	No detection	99%	0%	-	-
S190630ag	BBH (94 %)	18:52:05.179550	HV off	-	0%	-	-
S190701ah	BBH (93 %)	20:33:06.577637	No detection	19%	0%	-	-
S190706ai	BBH (99 %)	22:26:41.344727	HV off	-	0%	-	-
S190707q	BBH (>99 %)	09:33:26.181226	No detection	76%	25%	LEG	3.8×10^{-6}
S190718y	Terrestrial (98 %)	14:35:12.067865	No detection	22%	10%	LEG	1.2×10^{-5}
S190720a	BBH (99 %)	00:08:36.704102	HV off	-	0%	-	-
S190727h	BBH (92 %)	06:03:33.985887	No detection	14%	0%	-	-
S190728q	MassGap (52 %)	06:45:10.529205	Outside	0%	0%	-	-
S190814bv	NSBH (>99 %)	21:10:39.012957	Hv off	-	0%	-	-
Fermi GBM-190816	sub-threshold	21:22:13.027	No detection	66%	25%	HE	2.8×10^{-5}
S190828j	BBH (>99 %)	06:34:05.756472	No detection	28%	0%	-	-
S190828l	BBH (>99 %)	06:55:09.886557	No detection	79%	0%	-	-
S190901ap	BNS (86 %)	23:31:01.837767	No detection	82%	5%	LEG	2.8×10^{-5}
S190910d	NSBH (98 %)	01:26:19.242676	No detection	77%	0%	-	-
S190910h	BNS (61 %)	08:29:58.544448	No detection	78%	10%	LEG	5.3×10^{-7}
S190915ak	BBH (>99 %)	23:57:02.690891	No detection	100%	0%	-	-
S190923y	NSBH (68 %)	12:55:59.645508	No detection	68%	0%	-	-
S190924h	MassGap (> 99 %)	02:18:46.846654	HV off	-	0%	-	-
S190930s	MassGap (95 %)	13:35:41.246810	No detection	100%	5%	HE	4.5×10^{-5}
S190930t	NSBH (74 %)	14:34:07.685342	No detection	74%	0%	-	-
S191105e	BBH (95 %)	14:35:21.933105	HV off	-	0%	-	-
S191109d	BBH (>99 %)	01:07:17.220703	HV off	-	0%	-	-
S191129u	BBH (>99 %)	13:40:29.197372	No detection	70%	0%	-	-
S191204r	BBH (>99 %)	17:15:26.091822	No detection	4%	0%	-	-
S191205ah	NSBH (93 %)	21:52:08.568738	HV off	-	0%	-	-
S191213g	BNS (77 %)	04:34:08.142224	No detection	71%	5%	LEG	1.5×10^{-5}
S191215w	BBH (>99 %)	22:30:52.333152	No detection	83%	0%	-	-
S191216ap	BBH (>99 %)	21:33:38.472999	No detection	40%	0%	-	-
S191222n	BBH (>99 %)	03:35:37.119478	No detection	60%	0%	-	-
S200105ae	Terrestrial (97 %)	16:24:26.057208	No detection	67%	45%	HE	3.1×10^{-5}
S200112r	BBH (>99 %)	15:58:38.093931	No detection	67%	5%	HE	1.1×10^{-6}
S200114f	-	02:08:18.239300	HV off	-	85%	HE	1.2×10^{-5}
S200115j	MassGap (>99 %)	04:23:09.742047	HV off	-	15%	HE	8.5×10^{-5}
S200128d	BBH (97 %)	02:20:11.903320	No detection	60%	5%	HE	4.5×10^{-6}
S200129m	BBH (>99 %)	06:54:58.435104	HV off	-	5%	HE	4.8×10^{-4}
S200208q	BBH (>99 %)	13:01:17.991118	HV off	-	0%	-	-
S200213t	BNS (63 %)	04:10:40.327981	No detection	18%	0%	-	-
S200219ac	BBH (96 %)	09:44:15.195312	No detection	71%	0%	-	-
S200224ca	BBH (>99 %)	22:22:34.405762	HV off	-	95%	HE	9.0×10^{-7}
S200225q	BBH (96 %)	06:04:21.396973	HV off	-	0%	-	-
S200302c	BBH (89 %)	01:58:11.519119	No detection	81%	0%	-	-
S200311bg	BBH (>99 %)	11:58:53.397788	HV off	-	0%	-	-
S200316bj	MassGap (>99 %)	21:57:56.157221	No detection	90%	0%	-	-

Table 3: Summary of follow-up observation for gravitational wave events in O3

files to the public web server [19]. Also, the background estimation method for CGBM analysis was improved. While the background rate was estimated by averaged counts before and after the foreground integration time in the analysis for O3, the background was estimated by fitting count rates with a polynomial function of time in O4. The improved method can reduce the overestimation and underestimation of the background count rate. The analysis pipelines have been working stably since the first public alert was distributed on May 18, enabling us to check many gravitational wave events. Table 4 shows gravitational wave events reported by LIGO/Virgo/KAGRA collaboration in O4 in the same manner as Table 3. Although 169 gravitational events have been reported via the

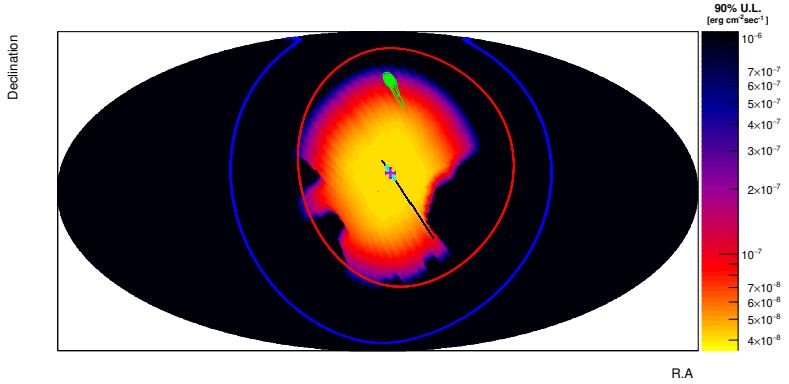

Figure 1: 90 % confidence level upper limits observed by CAL in the energy range 1 - 10 GeV during the interval ±60 s around the time of GW 190408an reported by LIGO/Virgo. Intensity scale is given in units of ergs cm^{-2} s^{-1}. Green contour is the LIGO/Virgo high probability region. Magenta cross marks the pointing direction of CAL at T_0, and the track of the pointing direction is marked cyan broad line in the interval ±60 s . Red and blue circles are the HXM and SGM fields of view ignoring effects of the ISS structures, respectively.

Event name	Possible source	Event time (T_0)	CGBM observation	$P_{\rm h}$	Coverage	Run mode	90 % Upper limit [erg s^{-1} cm^{-2}]
S230518h	NSBH (86%)	12:59:08	No detection	62%	0%	-	-
S230520ae	BBH (>99%)	22:48:42	No detection	61%	10 %	LEG	1.5×10^{-4}
S230522a	BBH (>99%)	09:38:05	HV off	-	-	-	-
S230522n	BBH (99%)	15:30:33	HV off	-	5 %	HE	1.5×10^{-6}
S230529ay	NSBH (62%)	18:15:00	HV off	-	15%	HE	6.5×10^{-5}
S230601bf	BBH (>99%)	22:41:34	HV off	-	15%	HE	1.6×10^{-3}
S230605o	BBH (99%)	06:53:43	No detection	69%	0%	-	-
S230606d	BBH (>99%)	00:43:05	No detection	100%	0%	-	-
S230608as	BBH (>99%)	20:50:47	No detection	100%	50%	LEG	5.0×10^{-5}
S230609u	BBH (96%)	06:49:58	No detection	87%	5%	LEG	4.2×10^{-5}
S230624av	BBH (95%)	11:31:03	HV off	-	0%	-	-
S230627c	NSBH (49%)	01:53:37	No detection	100%	0%	-	-
S230628ax	BBH (>99%)	23:12:00	HV off	-	0%	-	-
S230630am	BBH (98%)	12:58:06	HV off	-	40%	HE	3.3×10^{-4}
S230630bq	BBH (97%)	23:45:32	No detection	82%	10%	HE	1.5×10^{-3}

Table 4: Summary of follow-up observation for gravitational wave events in O4

GCN/LVC NOTICE and analyzed by the pipelines, only 15 significant events are shown in Table 4. CGBM and CAL searched for signals associated with 8 and 8 of 15 significant events, respectively. Figures 2 and 3 show count rate vs. time plots around T_0 of S230518h and S230627c likely black hole - neutron star mergers. No significant excess is seen in any detectors or channels in Figure 2 and 3. Including the other six events, there was no candidate in the CGBM data. Since there was no gamma-ray event associated with eight significant events in CAL data, upper limits were calculated, as well as O3 analysis. Figure 4 shows the 90 % confidence level upper limit map during the time interval $T_0\pm$ 60 s for S230529ay, which is a likely black hole - neutron star merger as an analysis example in O4.

4. Conclusion and Further prospective

CALET has searched for electromagnetic counterparts of gravitational wave events since observation started in October 2015. No candidate was associated with any gravitational wave events in CALET data as of the end of June. However, CGBM and CAL have a possibility of

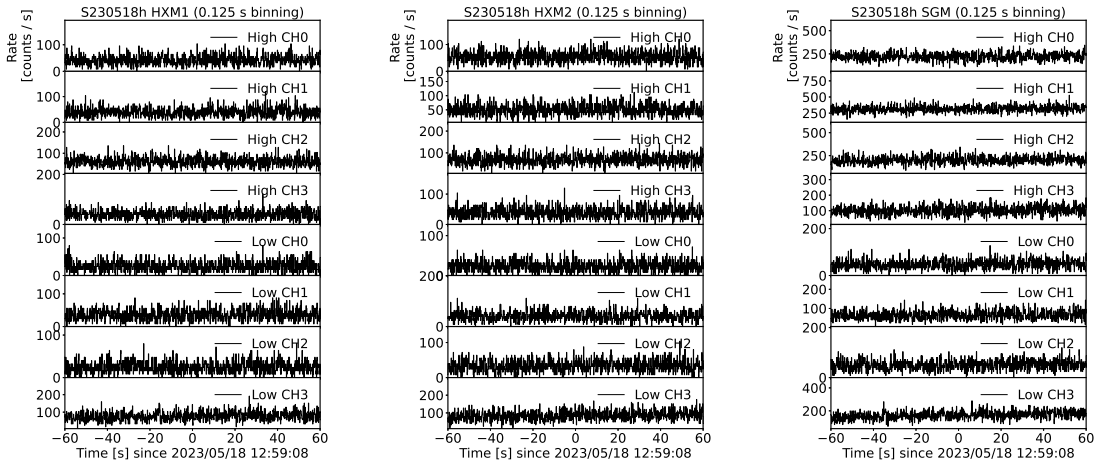

Figure 2: Time histories of counts detected by CGBM within ± 60 s of LIGO/Virgo event S230518h. No signal is seen in any detectors and channels.

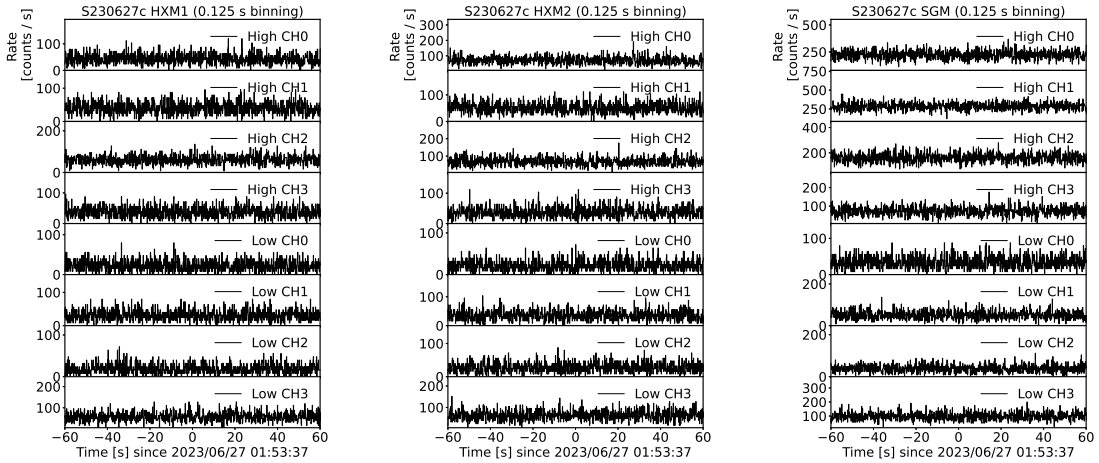

Figure 3: Time histories of counts detected by CGBM within ± 60 s of LIGO/Virgo event S230627c. No signal is seen in any detectors and channels.

detecting bright short GRBs associated with binary neutron star mergers. A significant binary neutron star merger has yet to be reported by LIGO/Virgo/KAGRA in O4. We are developing a new system to check CGBM data for GRBs detected by other GRB instruments. We developed a pipeline to check GCN Notices distributed by other GRB instruments and process quick-look analysis, which is similar to the CGBM pipeline for gravitational wave events. We have already implemented pipelines for checking GCN Notices by *Fermi*-GBM, *INTEGRAL* SPI-ACS, GECAM, and KONUS-*Wind*. We plan to implement pipelines for GCN Notices by *Swift*-BAT, and *Fermi*-LAT and MAXI/GSC to increase the possibility of detecting short GRBs associated with binary neutron star mergers.

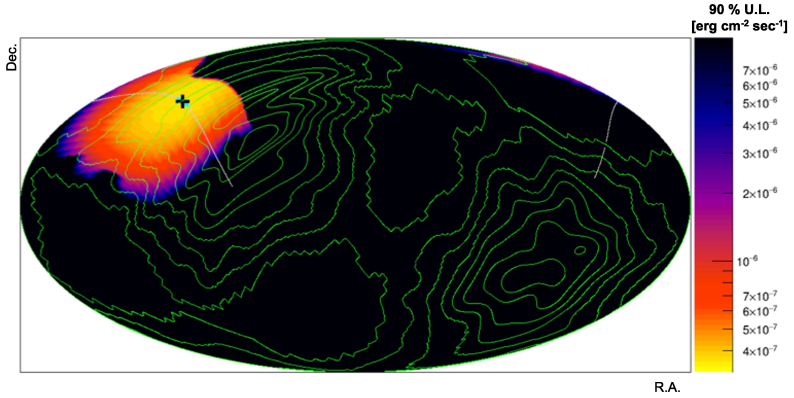

Figure 4: 90 % confidence level upper limits observed by CAL in the energy range 10 - 100 GeV during the interval ±60 s around the time of S230529ay reported by LIGO/Virgo/KAGRA. The intensity scale is given in units of ergs cm^{-2} s^{-1}. Green contour is the LIGO/Virgo high probability region. Black cross marks the pointing direction of CAL at T_0 and the track of the pointing direction is marked cyan broad line in the interval ±60 s.

Acknowledgment

We gratefully acknowledge JAXA's contributions to the development of CALET and to the operations onboard the International Space Station. The CALET effort in Italy is supported by ASI under Agreement No. 2013-018-R.0 and its amendments. The CALET effort in the United States is supported by NASA through Grants No. 80NSSC20K0397, No. 80NSSC20K0399, and No. NNH18ZDA001N-APRA18-0004. This work is supported in part by JSPS Grant-in-Aid for Scientific Research (S) Grant No. 19H05608 in Japan. A part of this research is made possible by use of data obtained from DARTS at ISAS/JAXA.

References

[1] B. P. Abbott et al., *GW170817: Observation of Gravitational Waves from a Binary Neutron Star Inspiral*, *PHYSICAL REVIEW LETTERS*, **119**, 161101, (2017).

[2] B. P. Abbott et al., *Multi-messenger Observations of a Binary Neutron Star Merger*, *The Astrophysical Journal Letters*, **848**, L12, (2017).

[3] V. Savchenko et al., *NTEGRAL Detection of the First Prompt Gamma-Ray Signal Coincident with the Gravitational-wave Event GW170817*, *The Astrophysical Journal Letters*, **848**, L15, (2017).

[4] A. Goldstein et al., *An Ordinary Short Gamma-Ray Burst with Extraordinary Implications: Fermi-GBM Detection of GRB 170817A*, *The Astrophysical Journal Letters*, **848**, L14, (2017).

[5] S. Torii et al., *Highlights from the CALET observations for 7.5 years on the International Space Station*, in this conference.

[6] T. Tamura et al., *Status of the operations of CALET for eight years on the International Space Station*, in this conference.

[7] O. Adriani et al., *CALET UPPER LIMITS ON X-RAY AND GAMMA-RAY COUNTERPARTS OF GW151226*, *The Astrophysical Journal Letters*, **829**, L20, (2016).

[8] K. Yamaoka et al., *CALET GBM Observations of Gamma-ray Bursts and Gravitational Wave Sources Proc.35th ICRC (Bexco, Busan, Korea, 2017)*, POS(ICRC2017), 614, (2017).

[9] O. Adriani et al., *Search for GeV Gamma-Ray Counterparts of Gravitational Wave Events by CALET*, *The Astrophysical Journal*, **863**, 160, (2018).

[10] M. Mori & Y. Asaoka for the CALET Collaboration, *High-Energy Gamma-ray Observations Using the CALorimetric Electron Telescope (CALET) on the ISS*, *Proc.36th ICRC (Madison, USA, 2019)*, POS(ICRC2019), 586, (2019).

[11] O. Adriani et al., *CALET Search for electromagnetic counterparts of gravitational waves during the LIGO/Virgo O3 run*, *The Astrophysical Journal*, **933**, 85, (2022).

[12] K. Yamaoka et al., *The CALET Gamma-ray Burst Monitor (CGBM)) Proc. 7th Huntsville Gamma-Ray Burst Symposium (Nashville, USA, 2013)*, paper 41 in eConf Proceedings C1304143, (2013).

[13] Y. Kawakubo et al., *Gamma-ray burst observation & gravitational wave event follow-up with CALET on the International Space Station Proc.37th ICRC (Online - Berlin, Germany, 2021)*, POS(ICRC2021), 957, (2021).

[14] N. Cannady et al., *Characteristics and Performance of the CALorimetric Electron Telescope (CALET) Calorimeter for Gamma-Ray Observations*, *The Astrophysical Journal Supplement Series*, **238**, 5, (2018)

[15] N. Cannady et al., *Refinement of the High-Energy Gamma-ray Selection for CALET on the International Space Station*, in this conference.

[16] M. Mori et al., *Results from CALorimetric Electron Telescope (CALET) Observations of Gamma-rays on the International Space Station*, in this conference.

[17] GraceDB, `https://gracedb.ligo.org`

[18] The General Coordinates Network, `https://gcn.nasa.gov`

[19] CGBM observation for GW events in O4, `http://cgbm.calet.jp/cgbm_trigger/O4/`

Full Author List: CALET Collaboration

O. Adriani[1,2], Y. Akaike[3,4], K. Asano[5], Y. Asaoka[5], E. Berti[2,6], G. Bigongiari[7,8], W.R. Binns[9], M. Bongi[1,2], P. Brogi[7,8], A. Bruno[10], N. Cannady[11,12,13], G. Castellini[6], C. Checchia[7,8], M.L. Cherry[14], G. Collazuol[15,16], G.A. de Nolfo[10], K. Ebisawa[17], A.W. Ficklin[14], H. Fuke[17], S. Gonzi[1,2,6], T.G. Guzik[14], T. Hams[11], K. Hibino[18], M. Ichimura[19], K. Ioka[20], W. Ishizaki[5], M.H. Israel[9], K. Kasahara[21], J. Kataoka[22], R. Kataoka[23], Y. Katayose[24], C. Kato[25], N. Kawanaka[20], Y. Kawakubo[14], K. Kobayashi[3,4], K. Kohri[26], H.S. Krawczynski[9], J.F. Krizmanic[12], P. Maestro[7,8], P.S. Marrocchesi[7,8], A.M. Messineo[8,27], J.W. Mitchell[12], S. Miyake[28], A.A. Moiseev[29,12,13], M. Mori[30], N. Mori[2], H.M. Motz[18], K. Munakata[25], S. Nakahira[17], J. Nishimura[17], S. Okuno[18], J.F. Ormes[31], S. Ozawa[32], L. Pacini[2,6], P. Papini[2], B.F. Rauch[9], S.B. Ricciarini[2,6], K. Sakai[11,12,13], T. Sakamoto[33], M. Sasaki[29,12,13], Y. Shimizu[18], A. Shiomi[34], P. Spillantini[1], F. Stolzi[7,8], S. Sugita[33], A. Sulaj[7,8], M. Takita[5], T. Tamura[18], T. Terasawa[5], S. Torii[3], Y. Tsunesada[35,36], Y. Uchihori[37], E. Vannuccini[2], J.P. Wefel[14], K. Yamaoka[38], S. Yanagita[39], A. Yoshida[33], K. Yoshida[21], and W.V. Zober[9]

[1]Department of Physics, University of Florence, Via Sansone, 1 - 50019, Sesto Fiorentino, Italy, [2]INFN Sezione di Firenze, Via Sansone, 1 - 50019, Sesto Fiorentino, Italy, [3]Waseda Research Institute for Science and Engineering, Waseda University, 17 Kikuicho, Shinjuku, Tokyo 162-0044, Japan, [4]JEM Utilization Center, Human Spaceflight Technology Directorate, Japan Aerospace Exploration Agency, 2-1-1 Sengen, Tsukuba, Ibaraki 305-8505, Japan, [5]Institute for Cosmic Ray Research, The University of Tokyo, 5-1-5 Kashiwa-no-Ha, Kashiwa, Chiba 277-8582, Japan, [6]Institute of Applied Physics (IFAC), National Research Council (CNR), Via Madonna del Piano, 10, 50019, Sesto Fiorentino, Italy, [7]Department of Physical Sciences, Earth and Environment, University of Siena, via Roma 56, 53100 Siena, Italy, [8]INFN Sezione di Pisa, Polo Fibonacci, Largo B. Pontecorvo, 3 - 56127 Pisa, Italy, [9]Department of Physics and McDonnell Center for the Space Sciences, Washington University, One Brookings Drive, St. Louis, Missouri 63130-4899, USA, [10]Heliospheric Physics Laboratory, NASA/GSFC, Greenbelt, Maryland 20771, USA, [11]Center for Space Sciences and Technology, University of Maryland, Baltimore County, 1000 Hilltop Circle, Baltimore, Maryland 21250, USA, [12]Astroparticle Physics Laboratory, NASA/GSFC, Greenbelt, Maryland 20771, USA, [13]Center for Research and Exploration in Space Sciences and Technology, NASA/GSFC, Greenbelt, Maryland 20771, USA, [14]Department of Physics and Astronomy, Louisiana State University, 202 Nicholson Hall, Baton Rouge, Louisiana 70803, USA, [15]Department of Physics and Astronomy, University of Padova, Via Marzolo, 8, 35131 Padova, Italy, [16]INFN Sezione di Padova, Via Marzolo, 8, 35131 Padova, Italy, [17]Institute of Space and Astronautical Science, Japan Aerospace Exploration Agency, 3-1-1 Yoshinodai, Chuo, Sagamihara, Kanagawa 252-5210, Japan, [18]Kanagawa University, 3-27-1 Rokkakubashi, Kanagawa, Yokohama, Kanagawa 221-8686, Japan, [19]Faculty of Science and Technology, Graduate School of Science and Technology, Hirosaki University, 3, Bunkyo, Hirosaki, Aomori 036-8561, Japan, [20]Yukawa Institute for Theoretical Physics, Kyoto University, Kitashirakawa Oiwake-cho, Sakyo-ku, Kyoto, 606-8502, Japan, [21]Department of Electronic Information Systems, Shibaura Institute of Technology, 307 Fukasaku, Minuma, Saitama 337-8570, Japan, [22]School of Advanced Science and Engineering, Waseda University, 3-4-1 Okubo, Shinjuku, Tokyo 169-8555, Japan, [23]National Institute of Polar Research, 10-3, Midori-cho, Tachikawa, Tokyo 190-8518, Japan, [24]Faculty of Engineering, Division of Intelligent Systems Engineering, Yokohama National University, 79-5 Tokiwadai, Hodogaya, Yokohama 240-8501, Japan, [25]Faculty of Science, Shinshu University, 3-1-1 Asahi, Matsumoto, Nagano 390-8621, Japan, [26]Institute of Particle and Nuclear Studies, High Energy Accelerator Research Organization, 1-1 Oho, Tsukuba, Ibaraki, 305-0801, Japan, [27]University of Pisa, Polo Fibonacci, Largo B. Pontecorvo, 3 - 56127 Pisa, Italy, [28]Department of Electrical and Electronic Systems Engineering, National Institute of Technology (KOSEN), Ibaraki College, 866 Nakane, Hitachinaka, Ibaraki 312-8508, Japan, [29]Department of Astronomy, University of Maryland, College Park, Maryland 20742, USA, [30]Department of Physical Sciences, College of Science and Engineering, Ritsumeikan University, Shiga 525-8577, Japan, [31]Department of Physics and Astronomy, University of Denver, Physics Building, Room 211, 2112 East Wesley Avenue, Denver, Colorado 80208-6900, USA, [32]Quantum ICT Advanced Development Center, National Institute of Information and Communications Technology, 4-2-1 Nukui-Kitamachi, Koganei, Tokyo 184-8795, Japan, [33]College of Science and Engineering, Department of Physics and Mathematics, Aoyama Gakuin University, 5-10-1 Fuchinobe, Chuo, Sagamihara, Kanagawa 252-5258, Japan, [34]College of Industrial Technology, Nihon University, 1-2-1 Izumi, Narashino, Chiba 275-8575, Japan, [35]Graduate School of Science, Osaka Metropolitan University, Sugimoto, Sumiyoshi, Osaka 558-8585, Japan, [36]Nambu Yoichiro Institute for Theoretical and Experimental Physics, Osaka Metropolitan University, Sugimoto, Sumiyoshi, Osaka 558-8585, Japan, [37]National Institutes for Quantum and Radiation Science and Technology, 4-9-1 Anagawa, Inage, Chiba 263-8555, Japan, [38]Nagoya University, Furo, Chikusa, Nagoya 464-8601, Japan, [39]College of Science, Ibaraki University, 2-1-1 Bunkyo, Mito, Ibaraki 310-8512, Japan